Geol. Mag. **148** (*5–6*), *2011, pp. 1009–1017.* © *Cambridge University Press 2011*
doi:10.1017/S0016756811000276

Kinematics of rock flow and fabric development associated with shear deformation within the Zagros transpression zone, Iran

ALI FAGHIH* & KHALIL SARKARINEJAD

Department of Earth Sciences, College of Sciences, Shiraz University, Shiraz, Iran

(*Received* 2 October 2010; *accepted* 13 January 2011; *first published online* 14 April 2011)

Abstract – This paper presents quantitative data on the finite strain, quartz crystal fabric, geometry of flow and deformation temperatures in deformed quartzite samples to characterize the ductile deformation along the thrust sheets constituting the Sanandaj–Sirjan Metamorphic Belt within the Zagros Mountains of Iran. The results of this study emphasize the heterogeneous nature of deformation in this belt, showing a spatial variation in strain magnitude and in degree of non-coaxiality. A dominant top-to-the-SE sense of shear is indicated by the asymmetry of microstructures and quartz c-axis fabrics. Quartz c-axis opening angles suggest deformation temperatures range between 435° ± 50 °C and 510° ± 50 °C, which yield greenschist to amphibolite facies conditions during the ductile deformation. Mean kinematic vorticity number (W_m) measured in the quartzite samples ranges between 0.6 and 0.9 with an average of 0.76, which indicates that extrusion of the metamorphic rocks of the region was facilitated by a significant component of pure shear strain. Traced towards the basal thrust of the Zagros Thrust System from northeast to southwest, the quartz grain fabrics change from asymmetric cross-girdle fabrics in the internal part of the deformation zone to an asymmetric single-girdle fabric at distances close to the basal thrust. This variation may depend on the structural depth and on the geometry of the ductile deformation zone. The observed increase in strain and vorticity within the study area is comparable with patterns recorded within metamorphic rock extrusions within other orogens in the world.

Keywords: quartz petrofabric, vorticity, deformation temperature, Sanandaj–Sirjan Metamorphic Belt, Zagros, Iran.

1. Introduction

Quartz is a common crustal mineral that undergoes crystal plastic deformation under a wide range of conditions, and there are many descriptions of its deformation microstructures and lattice preferred orientation (LPO) from a wide variety of metamorphic grades, strain geometries and finite strains. The analysis of these fabrics has been found to be useful in throwing light on understanding the active slip mechanism, the shape of the finite strain ellipsoid and the strain path (Law, Casey & Knipe, 1986; Platt & Behrmann, 1986; Law, 1990; Xypolias & Doutsos, 2000). As such, well-developed c-axis fabrics in natural tectonites can be used to characterize the kinematics of flow (Schmid & Casey, 1986; Sullivan & Law, 2007), the sense of shear (Law, 1990), the vorticity number associated with flow (Xypolias, 2009), the dominant deformation mechanisms during deformation (Lister & Dornsiepen, 1982) and the deformation temperature (Kruhl, 1996, 1998; Law, Searle & Simpson, 2004; Morgan & Law, 2004).

This paper presents quantitative data on strain, deformation temperature and vorticity of flow in the Sanandaj–Sirjan Metamorphic Belt of the Zagros Mountains of Iran and concludes with a discussion of the structural implication of the integrated strain, temperature and vorticity data. Our aim is the systematic collection of samples throughout the Sanandaj–Sirjan Metamorphic Belt in order to obtain estimates of the strain ratio and vorticity of flow at varying distances above the Zagros basal thrust. These data allow the identification of detailed geometric and kinematic constraints on the ductile transpression zone in which extrusion of medium- to high-grade metamorphic rocks has occurred. This belt is outlined by ductile transpressional deformation (Mohajjel & Fergusson, 2000; Sarkarinejad, Faghih & Grasemann, 2008; Sarkarinejad & Azizi, 2008; Sarkarinejad, Godin & Faghih, 2009; Sarkarinejad *et al.* 2010), which represents a crustal-scale shear zone accommodating deformation and displacement of metamorphic rocks during oblique collision between the Afro-Arabian continent and the Iranian microcontinents (Alavi, 1994).

2. Geological setting

The Zagros orogenic belt is part of the Alpine–Himalayan Mountain Range and extends for more than 1500 km in a NW–SE direction from eastern Turkey to the Minab Fault system in Southern Iran (Haynes & McQuillan, 1974; Stöcklin, 1974). The belt is considered to be a complex product of an early Mesozoic separation of the Iranian continental block from the rest of the Gondwana landmass

*Author for correspondence: afaghih@shirazu.ac.ir

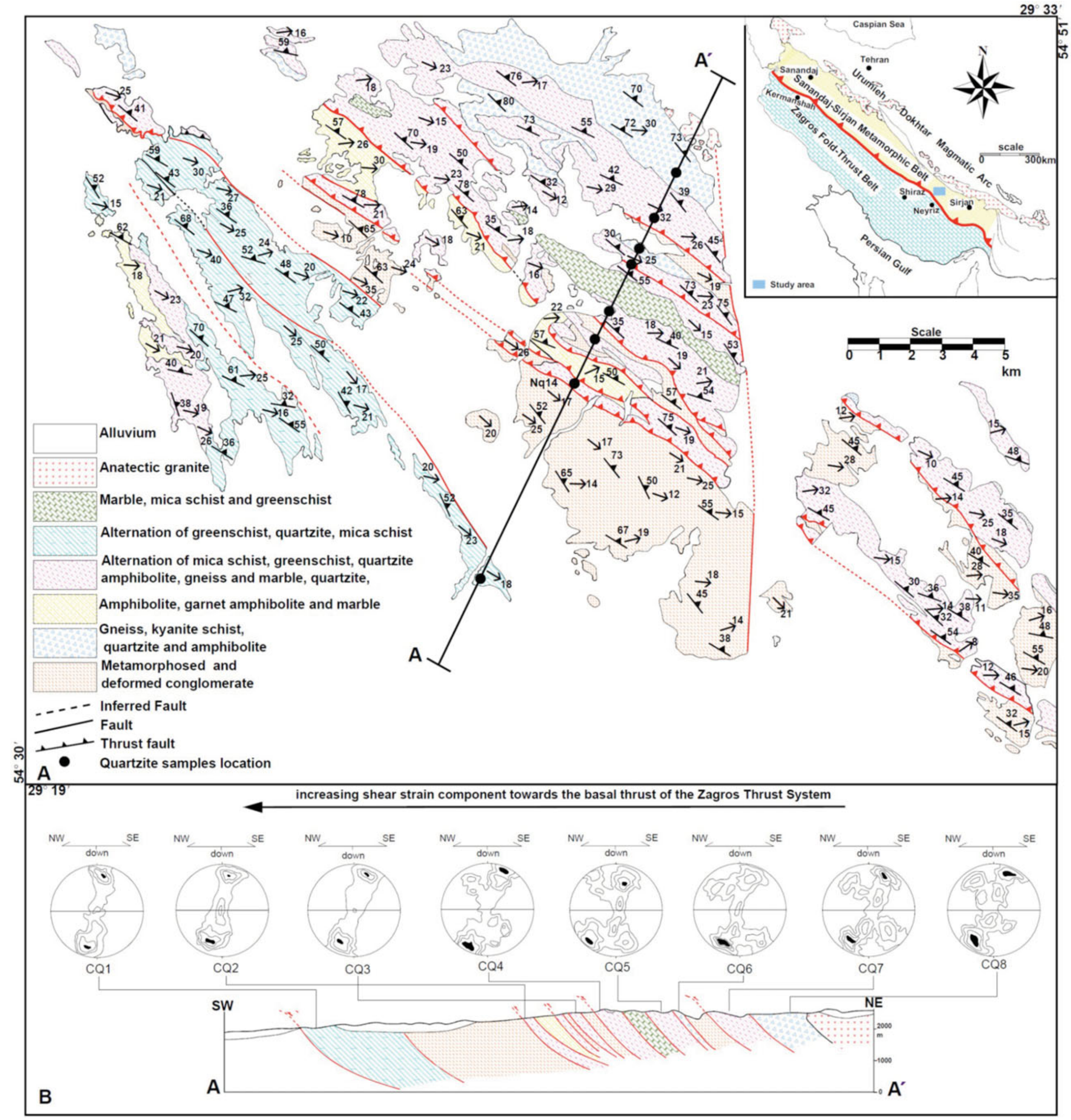

Figure 1. (Colour online) (a) Geological map of the study area. The inset map shows a tectonic map of Iran (modified after Alavi, 1994) with the Sanandaj–Sirjan Metamorphic Belt and the location of the study area. (b) The NE–SW transverse cross-section (A–A′) which shows spatial variation of lower hemisphere, equal-area projection of the quartz c-axis fabrics in the study area. The location of the quartzite samples and NE–SW transverse line are displayed in (a). In all these projections, the foliation is vertical and stretching lineation within the foliation is sub-horizontal.

followed by a NE-dipping subduction of the newly generated Neo-Tethyan oceanic crust below the Iranian microcontinents and subsequent collision between the Afro-Arabian and Iranian microcontinents (Alavi, 1994). The Late Cretaceous to Tertiary convergence between the Afro-Arabian continent and Iranian microcontinents accounts for thrusting and large-scale strike-slip faulting associated with crustal shortening in the Zagros orogeny (Alavi, 1994; Mohajjel & Fergusson, 2000; Sepehr & Cosgrove, 2005; Lacombe *et al*. 2006). Collision is still an ongoing orogenic process (Talebian & Jackson, 2002; Tatar, Hatzfeld & Ghafory-Ashtiyani, 2004; Allen, Jackson & Walker, 2004; Regard *et al*. 2004; Vernant *et al*. 2004; Authemayou *et al*. 2005) with a N–S-directed convergence rate of approximately 20 ± 2 mm yr^{-1} (Vernant *et al*. 2004).

A number of structural subdivisions are classically recognized in the Zagros Mountains. Starting from the southwest (Fig. 1), the Persian Gulf and Mesopotamian Plain represent the foredeep developed at the front of the orogen and thinning out progressively towards the southwest in the Arabian Platform. To the northeast, the Zagros fold–thrust belt consists of large parallel concentric folds related to Neogene inversion of the former Arabian passive margin (Alavi, 1994, 2004). The range is typically 250–350 km wide, from a southwestern margin along the edge of the Mesopotamian foreland and the Persian Gulf to the edge of the Turkish–Iranian Plateau in the northeast. The Zagros fold–thrust belt is bounded to the northeast by the Sanandaj–Sirjan Metamorphic Belt, consisting mainly of Precambrian metamorphic rocks, and the Urumieh–Dokhtar Magmatic Belt, an Andean-type volcanic magmatic arc including rocks ranging in age from Late Jurassic to Quaternary (Molinaro *et al*. 2005; Molinaro, Zeyen & Laurencin, 2005). The Sanandaj–Sirjan Metamorphic Belt is a zone of polyphase deformation, the latest reflecting the collision of the Afro-Arabian continent and Iranian microcontinents and subsequent southward propagation of the fold–thrust belt (Alavi, 1994). This part of the Zagros orogenic belt is 150–200 km wide and more than 1500 km long from the northwest (Sanandaj) to southeast (Sirjan) in the western part of Iran, which runs parallel to and is part of the NW–SE structural grain of the Zagros Mountains. Crustal shortening associated with subduction and collision metamorphosed and deformed late Palaeozoic and Mesozoic rocks in this zone. The Sanandaj–Sirjan Metamorphic Belt is a zone of thrust faults that have transported numerous slices of variously metamorphosed Phanerozoic stratigraphic units. Stratigraphic evidence and synorogenic conglomerates indicate that thrusting initiated in Late Cretaceous time (Alavi, 1994). The study area is located in the Neyriz area, 300 km southeast from Shiraz in southern Iran. Metamorphosed and deformed rocks of this area are part of the Sanandaj–Sirjan Metamorphic Belt (Fig. 1).

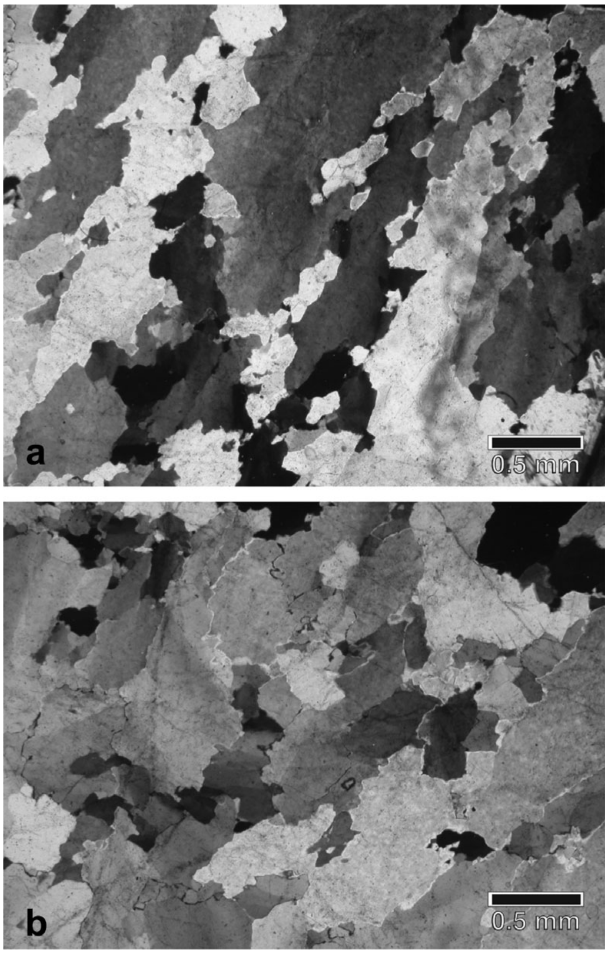

Figure 2. Photomicrograph of quartz mylonites from the Sanandaj–Sanandaj Metamorphic Belt in the study area. Elongate and plastically deformed quartz grains form a well-developed shape-preferred orientation. The quartz grains record evidence of dynamic recrystallization by subgrain rotation and grain boundary migration. (a) Relicts of large old quartz grains with undulose extinction and elongate subgrains pass laterally into domains of small, new grains. (b) Polycrystalline quartz with irregular grain boundaries formed in response to grain boundary migration recrystallization. For example, the dark grain is bulging into the light-grey grain in the central part of the image.

3. Microstructures and quartz c-axis fabrics

In order to constrain the kinematics of the shearing event, quartz c-axis fabric measurements were carried out on eight deformed quartzite samples selected from different structural positions and located along a NE–SW transverse line across the Sanandaj–Sirjan Metamorphic Belt. Quartzite samples have been used for the measurements and the evaluation of lattice preferred orientation. C-axis orientations of 300 or more quartz grains from each specimen from the study area were measured on sections cut parallel to the lineation and perpendicular to the foliation. The analyses of quartz c-axis fabrics were made using an optical microscope equipped with a universal stage located in Shiraz University, Department of Earth Sciences. The c-axis measurements are displayed on equal-area, lower hemisphere stereographic projections. The mesoscopic foliation plane, its normal and the stretching lineation lying on foliation define a reference coordinate frame.

Most of the collected samples record a well-preserved shape and lattice preferred orientation (Fig. 2). The fabric of the dynamically recrystallized quartz was formed by both subgrain rotation and grain boundary migration. Generally, the presence of a lattice preferred orientation is interpreted as evidence for deformation by dislocation glide and creep (Vernooij, Brok & Kunze, 2006). From the density distribution of quartz c-axes, the fabrics of the study area can be described as single-girdle and Type-I cross-girdle fabrics, which are oblique to the foliation trend indicating the operation of non-coaxial shearing during deformation (Lister, 1977; Lister & Hobbs, 1980; Schmid & Casey, 1986; Law, 1990). Deformation geometry and shear sense are deduced from methods described by Simpson & Schmid (1983), Ramsay & Huber (1987), Law (1990) and Bell & Johnson (1992). The top-to-the-SE sense of shear is confirmed by microstructures and microtextures. These c-axis fabrics show an obliquity of the central girdle segment (ψ) with respect to the main foliation and lineation, indicating a non-coaxial top-to-the-SE sense of shear (Fig. 3; Table 1). The obliquity of the

https://doi.org/10.1017/S0016756811000276 Published online by Cambridge University Press

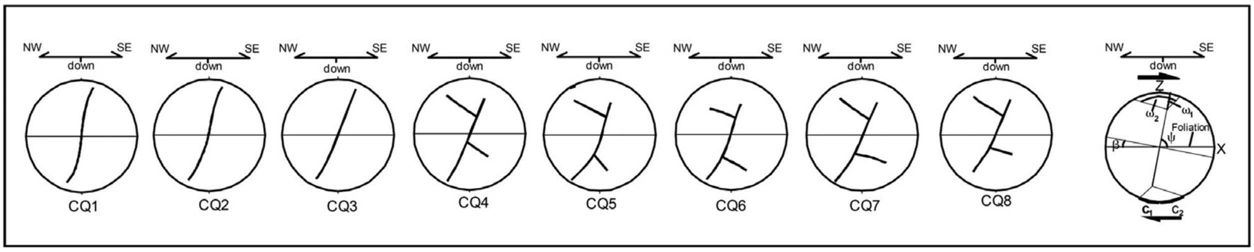

Figure 3. The fabric skeletons and angular relationships between quartz c-axis external and internal fabric asymmetry that is used in this paper. The parameters used to define external and internal fabric asymmetry are illustrated. The observed fabric asymmetry indicates a significant component of non-coaxial, top-to-the-SE sense of shear.

Table 1. Petrofabric, strain and vorticity data for quartzite samples from the study area

Sample	Quartz c-axis fabric asymmetry parameters (degree)					Finite strain analysis	Vorticity analysis
	ψ	c_1	c_2	ω_1	ω_2		
CQ1	79	12	58	24	83	6.0	0.90
CQ2	79	11	52	22	87	4.5	0.86
CQ3	82	10	51	19	87	3.8	0.82
CQ4	80	9	56	19	88	3.6	0.78
CQ5	76	18	35	38	85	3.4	0.73
CQ6	77	16	60	31	91	3.2	0.71
CQ7	71	6	66	8	90	3.1	0.66
CQ8	75	12	31	26	89	2.8	0.60

central girdle segment (external asymmetry parameter) varies between 71° and 82°. Almost all the c-axis fabrics exhibit monoclinic peripheral point-maxima asymmetry with respect to the foliation, which is consistent with the pattern commonly reported for non-coaxial deformation (Wang *et al.* 2005). Fabric skeletons were prepared from the contoured fabric diagrams by connecting the crests and ridges (Lister & Williams, 1979; Lister & Hobbs, 1980; Vissers, 1989; Joy & Saha, 2000). External fabric asymmetry may also be expressed by the relative magnitudes of the parameters c_1 and c_2 within individual samples (Platt & Behrmann, 1986; Law, 1987, 1990; Law, Knipe & Dayan, 1984). Within the quartzite samples, c_1 is smaller than c_2 indicating a top-to-the-SE sense of shear. The same sense of shear may be expressed by the relative magnitudes of ω_1 and ω_2 (internal asymmetry), where ω_2 is consistently greater than ω_1 in each sample (Fig. 3; Table 1).

4. Finite strain analysis

Finite strain ratio in the XZ plane (R_{XZ}) was estimated using the R_f/φ method (Ramsay, 1967; Lisle, 1985) on the elliptical strain markers such as plastically deformed quartz grains in the deformed quartzites of the study area (Table 1). The R_f/φ method can yield unreliable results on specimens in which repeated recrystallization has significantly modified the original shape of the observed quartz grains. Therefore, thin-sections in which quartz grains showed no evidence of recrystallization were chosen for the finite strain analysis. For each thin-section, strain markers were traced on transparent overlays on the enlarged photomicrographs. At least 80 deformed quartz grains were digitized from enlarged photographs of thin-sections in each sample and then R_f/φ diagrams were constructed manually. It is emphasized that strain analysis was not attempted on pure quartzites owing to the fact that in these rocks the aspect ratio of quartz grains was significantly modified by dynamic recrystallization.

5. Degree of non-coaxiality

The analysis of kinematic indicators in the study area reveals differences in quartz c-axis asymmetry, reflecting spatial partitioning of the flow between domains that underwent coaxial flow and those that underwent non-coaxial flow. Quantitative determination of the vorticity is extremely valuable when attempting to reconstruct a deformation because it describes the degree of non-coaxiality of flow, or the relative amounts of pure versus simple shear, and helps to define the kinematic reference frame for the flow in ductile shear zones (Grasemann, Fritz & Vannay, 1999; Law, Searle & Simpson, 2004; Carosi *et al.* 2006; Jessup *et al.* 2006; Short & Johnson, 2006; Forte & Bailey, 2007). The kinematic vorticity number (W_K) is a dimensionless number that describes this quality of flow, where pure shear is described by $W_K = 0$, and simple shear is described by $W_K = 1$. General shear is the term used for flows intermediate between the pure and simple shear end members, in which $1 > W_K > 0$ (Passchier & Trouw, 2005). Pure and simple shearing components contribute equally to the instantaneous flow at $W_K = 0.71$ (Law, Searle & Simpson, 2004). In natural systems the vorticity of flow may vary with both position and time (Fossen & Tikoff, 1993, 1998). However, to integrate the vorticity of the flow (W_K) over time and space it is more appropriate to consider the mean vorticity number W_m (Passchier, 1988).

The approximately plane-strain condition which is suggested from the cross-girdle pattern of the quartz c-axis fabrics (Law, 1990) satisfies the application of two-dimensional vorticity analysis (Tikoff & Fossen, 1995). In this work, a method based on quartz fabrics proposed by Wallis (1992, 1995) is used in order to estimate W_m. This method is based on measuring Type-I (Lister, 1977) cross-girdle quartz c-axis fabrics and strain ratios in the XZ plane of finite strain. The angle

https://doi.org/10.1017/S0016756811000276 Published online by Cambridge University Press

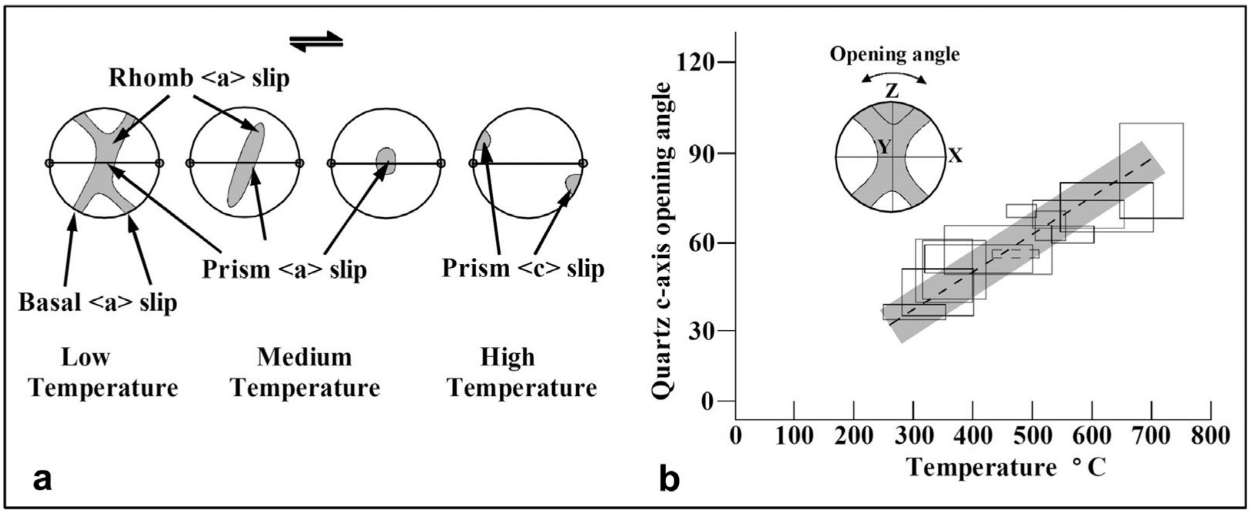

Figure 4. Quartz lattice preferred orientations (LPO) and associated temperature indicators. (a) Simplified stereonets showing dependence of quartz LPOs and inferred slip systems on increasing temperature (modified from Passchier & Trouw, 2005). (b) Graph of the quartz c-axis fabric opening angles versus estimated temperatures of deformation for eight quartzite samples of naturally deformed rocks in the Neyriz area showing effect of temperature on the opening angle of small-circles of the quartz c-axes in an LPO diagram (after Kruhl, 1996, 1998; Law, Searle & Simpson, 2004; Morgan & Law, 2004). Fabric opening angle is defined in inset diagram. All boxes (except one with dashed lines, which shows data from this research) indicate data taken from the literature (Kruhl, 1996, 1998; Law *et al*. 1992; Okudaira *et al*. 1995).

β between the perpendicular to the central girdle of the quartz c-axis diagram and the foliation is equal to the angle between the flow plane and the principal plane of normal strain in this method. This angle is a function of R_{XZ} and W_m, as described by Wallis (1995):

$$W_m = \sin\left\{\tan^{-1}\left[\frac{\sin(2\beta)}{[(R_{XZ}+1)/(R_{XZ}-1)] - \cos(2\beta)}\right]\right\} \times \frac{(R_{XZ}+1)}{(R_{XZ}-1)} \quad (1)$$

This method was applied to the deformed samples where asymmetric quartz c-axis fabrics are observed. The analysis of samples from the study area yielded values of W_m in the range 0.6–0.9 (Table 1).

6. Deformation temperature

During plastic deformation and dynamic crystallization, increased temperature results in an increased opening angle of peripheral legs of quartz c-axis fabrics (Tullis, Christie & Griggs, 1973; Lister & Hobbs 1980; Lister & Dornsiepen 1982). The relationship between the opening angle of quartz c-axis fabrics and deformation temperatures is linear through greenschist to upper amphibolite facies conditions (Kruhl, 1996, 1998; Law, Searle & Simpson, 2004). In the case of plane strain deformation this opening angle is defined as the angle between the two c-axis girdles measured in the plane perpendicular to the foliation and parallel to the lineation. The basic assumption made in using this geothermometer is that the range in strain rates and effects of hydrolytic weakening likely to be encountered in natural deformation is encompassed in the geothermometer. For natural deformation this opening angle thermometer may give deformation temperatures with an uncertainty of ±50 °C (Law, Searle & Simpson, 2004). In order to estimate temperatures during ductile deformation of the analysed deformed quartzites, the geothermometer of Kruhl (1996, 1998) modified by Law, Searle & Simpson (2004) and Morgan & Law (2004) was used. The asymmetric crossed girdles display opening angles ranging from 55° to 75°. Using this modified geothermometer the fabric opening angles indicate that deformation temperature varies from 435° ± 50 °C to 510° ± 50 °C in the study area (Fig. 4).

7. Thinning and dip-parallel elongation

Deviation from ideal simple shear deformation implies thinning of the Sanandaj–Sirjan Metamorphic Belt perpendicular to the deformation zone boundaries (flow plane) and resultant dip-parallel elongation. For plane strain deformation, the stretch magnitude both normal and parallel to the flow plane can be calculated. In order to study the importance of the deviation from simple shear within the study area, the stretch magnitude both normal and parallel to the flow plane was calculated combining strain and vorticity data by using the mathematical expression suggested by Wallis, Platt & Knott (1993):

$$S = \left\{\frac{1}{2}(1-W_K^2)^{1/2}\left[\left(R_{XZ}+R_{XZ}^{-1}+2\frac{(1+W_K^2)}{(1-W_K^2)}\right)^{1/2} + (R_{XZ}+R_{XZ}^{-1}-2)^{1/2}\right]\right\}^{-1} \quad (2)$$

https://doi.org/10.1017/S0016756811000276 Published online by Cambridge University Press

where S is stretch perpendicular to the deformation zone. Integration of strain and vorticity data yields dip-parallel elongation between 25 % and 80 % and thinning perpendicular to the flow plane between 22 % and 44 %.

8. Discussion

The microscope-based and detailed skeletal fabric parameter analyses indicate that subtle fabric asymmetries are consistent with a top-to-the-SE sense of shear. Strong c-axis fabrics were observed in all samples and can be divided into two groups: (i) single girdles with an asymmetric distribution with respect to the foliation; (ii) a cross girdle with an asymmetric distribution with respect to the foliation. These different groups may reflect different strain histories, with the asymmetric c-axis recording a non-coaxial deformation history (Lister, 1977; Lister & Hobbs, 1980). The sense of asymmetry observed in the c-axis fabrics is consistent with other observed microscopic and mesoscopic kinematic indicators (Fig. 5), which show top-to-the-SE sense of shear. Information about strain symmetry can be retrieved from the obtained quartz c-axis fabrics (Schmid & Casey 1986; Law, 1990). The crossed-girdle pattern of the quartz c-axis fabrics in the samples is interpreted to indicate approximately plane-strain conditions during top-to-the-SE ductile shearing.

Pattern geometry is primarily controlled by activity of different glide systems, which in turn are temperature sensitive. Both theoretical and experimental studies have indicated that c-axis fabric intensity increases with increasing finite strain (Hongn & Hippertt, 2001). The strain ratio increases systematically from the northeast to the southwest approaching a value of 6 close to the basal thrust of the Zagros Thrust System and a value of 2.8 in the inner parts of the study area. Similar integrated strain ratio changes have recently been reported for other convergent orogens including the Hellenides of Greece (Xypolias & Doutsos, 2000; Doutsos *et al.* 2000; Xypolias & Koukouvelas, 2001; Kokkalas & Doutsos, 2004), the Himalaya (Law, Searle & Simpson, 2004) and the European Alps (Ring & Kassem, 2007). The continuous evolution of cross-girdles to single-girdles has been interpreted as resulting from an increasing finite strain (Schmid & Casey, 1986). Quartz c-axis data show a continuous evolution from asymmetric cross-girdles to oblique single-girdles from northeast to southwest in the study area. The quartz c-axis fabric and kinematic vorticity number values might reflect a relative increase of the simple shear component towards the basal thrust of the Zagros Thrust System (i.e. from northeast to southwest).

Lattice preferred orientation in the quartz aggregates is an indicator of deformation temperature since the fabric pattern is controlled by the relative contributions of different slip systems, which in turn are temperature sensitive (Fig. 4a). Slip in the quartz occurs primarily in the <a> crystallographic direction, predominantly on the basal, rhomb and prism planes. Basal <a> slip is dominant at lower temperatures and at faster strain rates, causing a c-axis fabric maximum near the Z-axis of the finite strain ellipsoid. With increasing temperature, a rhombohedral <a> slip system becomes activated, causing a fabric maximum at an intermediate orientation between the Y- and Z-axes. Ultimately, at still higher temperature and slower strain rates, the prism <a> slip system operates, causing a fabric maximum near the Z-axis of the finite strain ellipsoid (Bouchez, 1977; Hobbs, 1985; Lister & Dornsiepen, 1982; Mainprice *et al.* 1986; Ralser, Hobbs & Ord, 1991; Schmid & Casey, 1986; Tullis, 1977; Tullis, Christie & Griggs, 1973). Using a modified geothermometer and estimates of mean temperature we propose that the quartzites of the northern parts of the study area were deformed under greenschist facies conditions whereas the quartzites close to the basal thrust were deformed under amphibolite facies conditions. The opening angles of the quartz fabrics

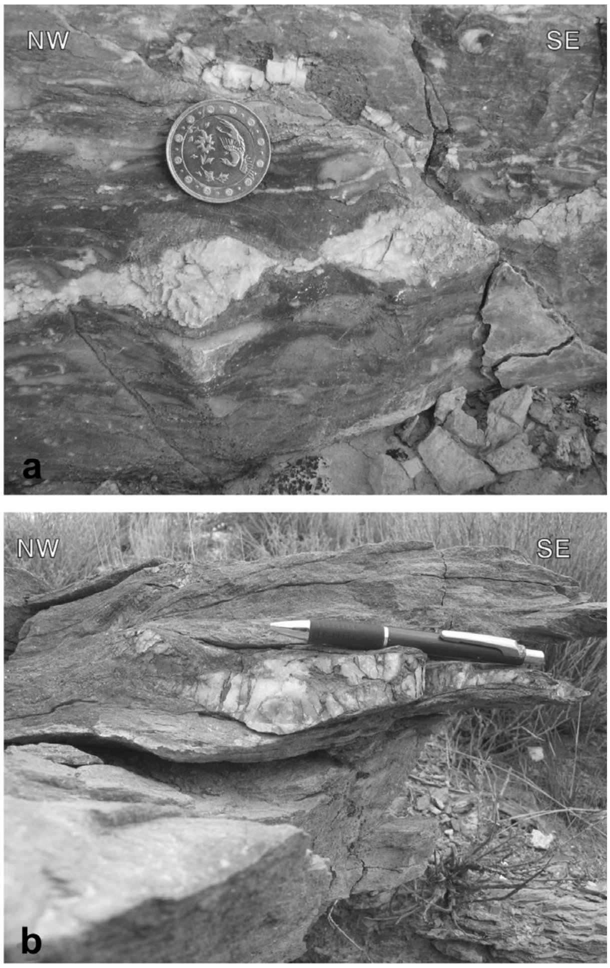

Figure 5. Mesoscopic kinematic indicators of the Sanandaj–Sirjan Metamorphic Belt which show top-to-the-SE sense of shear. (a) Boudin trains formed during shear deformation indicating top-to-the-SE sense of shear and a strong stretching component parallel to the shear zone boundary. Diameter of coin is approximately 20 mm. (b) Field photo of a sigmoidal-shaped quartz lens with monoclinic symmetry which shows top-to-the-SE sense of shear. Pen is approximately 14 cm long.

reveal that deformation temperature varies from 435 ± 50 °C within the northern parts of the study area to 510 ± 50 °C within the southern parts of the study area (Fig. 4b). The appearance of crossed-girdles in the northern parts of the study area indicates the dominance of basal <a> gliding, with less pronounced rhombohedral <a> and prism <a> gliding, which is common for deformation under low grade metamorphic conditions (Schmid & Casey, 1986; Law, 1990). According to the dependence of quartz lattice preferred orientations and inferred slip systems on increasing temperature (Passchier & Trouw, 2005), it seems that the southern parts of the study area experienced higher temperatures compared to the northern parts (Fig. 4a).

Using numerical relationships originally established by Wallis, Platt & Knott (1993), integration of the strain and vorticity data allows us to estimate the amount of shortening in the mylonitic quartzites within the Sanandaj–Sirjan Metamorphic Belt, measured perpendicular to the flow plane. For plane strain deformation, stretching parallel to the flow plane in the transport direction is simply the reciprocal of the shortening value. However, integrated strain and vorticity data indicate that vertical thinning and transport-parallel stretching were important tectonic processes during thrusting at the base of the Zagros Thrust. This suggests that nappe emplacement occurs by a combination of simple shear with a pure shear component of vertical flattening/shortening. Vertical thinning by penetrative deformation associated with combined pure and simple shear provides at least one mechanism for extrusion of deeper crustal rocks to shallower levels (Feehan & Brandon, 1999).

9. Conclusion

Extensive quantitative new structural, textural and quartz petrofabric analyses within the Sanandaj–Sirjan Metamorphic Belt reveal that mesoscopic and microscopic kinematic indicators show unequivocal top-to-the-SE sense of shear. Quantitative vorticity analyses in conjunction with quartz fabric data and microstructural analyses indicate that deformation within this belt involved general non-coaxial flow with contemporaneous contributions of pure and simple shear. The results of this study demonstrate that both strain ratio and the simple shear component of deformation increase towards the basal thrust of the Zagros Thrust System. The observed increase in strain and vorticity within the study area is comparable with patterns recorded within other orogens in the world.

Acknowledgements. The authors would like to thank the editors Mark Allen, Bernhard Grasemann, Guy Simpson and Olivier Lacombe for their editorial authority. We are grateful to Michael Edwards and an anonymous reviewer for helpful and valuable reviews of the manuscript. The Research Council of the Shiraz University (RCSU) has supported this study, which is gratefully acknowledged.

References

Alavi, M. 1994. Tectonics of the Zagros Orogenic belt of Iran: new data and interpretations. *Tectonophysics* **229**, 211–38.

Alavi, M. 2004. Regional stratigraphy of the Zagros fold-thrust belt of Iran, and its proforeland evolution. *American Journal of Science* **304**, 1–20.

Allen, M. B., Jackson, J. & Walker, R. 2004. Late Cenozoic reorganization of the Arabia-Eurasia collision and comparison of the short-term and long-term deformation rates. *Tectonics* **23**, TC2008, doi: 10.1029/2003TC001530, 16 pp.

Authemayou, C., Bellier, O., Chardon, D., Malekzade, Z. & Abassi, M. 2005. Role of the Kazerun fault system in active deformation of the Zagros fold-and-thrust belt, Iran. *Comptes Rendus Geoscience* **337**, 539–45.

Bell, T. H. & Johnson, S. E. 1992. Shear sense: a new approach that resolves conflicts between criteria in metamorphic rocks. *Journal of Metamorphic Geology* **10**, 99–124.

Bouchez, J. L. 1977. Plastic deformation of quartzites at low temperatures in an area of natural strain gradient. *Tectonophysics* **39**, 25–50.

Carosi, R., Montomoli, C., Rubatto, D. & Visona, D. 2006. Normal-sense shear zones in the core of the Higher Himalayan Crystallines (Bhutan Himalaya): evidence for extrusion? In *Channel Flow, Ductile Extrusion and Exhumation in Continental Collision Zones* (eds R. D. Law, M. P. Searle & L. Godin), pp. 425–44. Geological Society of London, Special Publication no. 268.

Doutsos, T., Koukouvelas, I., Poulimenos, G., Kokkalas, S., Xypolias, P. & Skourlis, K. 2000. An exhumation model of the south Peloponnesus, Greece. *International Journal of Earth Science* **89**, 350–65.

Feehan, J. & Brandon, M. T. 1999. Contribution of ductile flow to exhumation of low-T-high-P metamorphic rocks: San Juan-Cascade nappes, NW Washington State. *Journal of Geophysical Research* **104**, 10883–902.

Forte, A. M. & Bailey, C. M. 2007. Testing the utility of the porphyroclast hyperbolic distribution method of kinematic vorticity analysis. *Journal of Structural Geology* **29**, 983–1001.

Fossen, H. & Tikoff, B. 1993. The deformation matrix for simultaneous simple shearing, pure shearing and volume change, and its application to transpression–transtension tectonics. *Journal of Structural Geology* **15**, 413–22.

Fossen, H. & Tikoff, B. 1998. Extended models of transpression and transtension, and application to tectonic settings. In *Continental Transpressional and Transtensional Tectonics* (eds R. E. Holdsworth, R. A. Strachan, & J. F. Dewey), pp. 15–33. Geological Society of London, Special Publication no. 135.

Grasemann, B., Fritz, H. & Vannay, J. C. 1999. Quantitative kinematic flow analysis from the Main Central Thrust Zone (NW-Himalaya, India): implications for a decelerating strain path and the extrusion of orogenic wedges. *Journal of Structural Geology* **21**, 837–53.

Haynes, S. J. & McQuillan, H. 1974. Evolution of the Zagros suture zone, Southern Iran. *Geological Society of America Bulletin* **85**, 739–44.

Hobbs, B. E. 1985. The geological significance of microfabric. In *Preferred Orientation in Deformed Metals and Rocks* (ed. H. R. Wenk), pp. 463–84. New York: Academic Press.

Hongn, F. D. & Hippertt, J. F. 2001. Quartz crystallographic and morphologic fabrics during folding/transposition in mylonites. *Journal of Structural Geology* **23**, 81–92.

JESSUP, M. J., LAW, R. D., SEARLE, M. P. & HUBBARD, M. S. 2006. Structural evolution and vorticity of flow during extrusion and exhumation of the Greater Himalayan Slab, Mount Everest Massif, Tibet/Nepal: implications for orogen-scale flow partitioning. In *Channel Flow, Ductile Extrusion and Exhumation in Continental Collision Zones* (eds R. D. Law, M. P. Searle & L. Godin), pp. 379–414. Geological Society of London, Special Publication no. 268.

JOY, S. & SAHA, D. 2000. Dynamically recrystallised quartz c-axis fabrics in greenschist facies quartzites, Singhbhum shear zone and its footwall, eastern India – influence of high fluid activity. *Journal of Structural Geology* **22**, 777–93.

KOKKALAS, S. & DOUTSOS, T. 2004. Kinematics and strain partitioning in the southeast Hellenides (Greece). *Geological Journal* **39**, 121–40.

KRUHL, J. H. 1996. Prism- and basal-plane parallel subgrain boundaries in quartz; a microstructural geothermobarometer. *Journal of Metamorphic Geology* **14**, 581–9.

KRUHL, J. H. 1998. Reply: prism- and basal-plane parallel subgrain boundaries in quartz: a microstructural geothermobarometer. *Journal of Metamorphic Geology* **16**, 142–6.

LACOMBE, O., MOUTHEREAU, F., KARGAR, S. & MEYER, B. 2006. Late Cenozoic and modern stress fields in the western Fars (Iran): implications for the tectonic and kinematic evolution of central Zagros. *Tectonics* **25**, TC1003, doi: 10.1029/2005TC001831, 27 pp.

LAW, R. D. 1987. Heterogeneous deformation and quartz crystallographic fabric transitions: natural examples from the Moine Thrust zone at the Stack of Glencoul, northern Assynt. *Journal of Structural Geology* **9**, 819–34.

LAW, R. D. 1990. Crystallographic fabrics. A selective review of their applications to research in structural geology. In *Deformation Mechanisms, Rheology and Tectonics* (eds R. J. Knipe & E. H. Rutter), pp. 335–52. Geological Society of London, Special Publication no. 54.

LAW, R. D., CASEY, M. & KNIPE, R. J. 1986. Kinematic and tectonic significance of microstructures and crystallographic fabrics within quartz mylonites from the Assynt and Eriboll regions of the Moine thrust zone, NW Scotland. *Transactions of the Royal Society of Edinburgh: Earth Sciences* **77**, 99–125.

LAW, R. D., KNIPE, R. J. & DAYAN, H. 1984. Strain path partitioning within thrust sheets: microstructural and petrofabric evidence from the Moine Thrust zone at Loch Eriboll, northwest Scotland. *Journal of Structural Geology* **6**, 477–97.

LAW, R. D., MORGAN, S. S., CASEY, M., SYLVESTER, A. G., NYMAN, M. 1992. The Papoose Flat Pluton, California: a reassessment of its emplacement history in the light of new microstructural and crystallographic observations. *Transaction of the Royal Society of Edinburgh: Earth Sciences* **83**, 361–75.

LAW, R. D., SEARLE, M. P. & SIMPSON, R. L. 2004. Strain, deformation temperatures and vorticity of flow at the top of the Greater Himalayan Slab, Everest Massif, Tibet. *Journal of Geological Society, London* **161**, 305–20.

LISLE, R. J. 1985. *Geological Strain Analysis: A Manual for the Rf/φ Method*. New York: Pergamon Press, 99 pp.

LISTER, G. S. 1977. Crossed-girdle c-axis fabrics in quartzites plastically deformed by plane strain and progressive simple shear. *Tectonophysics* **39**, 51–4.

LISTER, G. S. & DORNSIEPEN, U. F. 1982. Fabric transitions in the Saxony granulite terrain. *Journal of Structural Geology* **41**, 81–92.

LISTER, G. S. & HOBBS, B. E. 1980. The simulation of fabric development during plastic deformation and its application to quartzite: the influence of deformation history. *Journal of Structural Geology* **2**, 355–71.

LISTER, G. S. & WILLIAMS, P. F. 1979. Fabric development in shear zones: theoretical controls and observed phenomena. *Journal of Structural Geology* **1**, 283–97.

MAINPRICE, D., BOUCHEZ, J. L., BLUMENFELD, P. & TUBIA, J. M. 1986. Dominant c-slip in naturally deformed quartz: implications for dramatic plastic softening at high temperature. *Geology* **14**, 819–22.

MOHAJJEL, M. & FERGUSSON, C. L. 2000. Dextral transpression in Late Cretaceous continental collision, Sanandaj–Sirjan Zone, western Iran. *Journal of Structural Geology* **22**, 1125–39.

MOLINARO, M., LETURMY, P., GUEZOU, J.-C., FRIZON DE LAMOTTE, D. & ESHRAGHI, S. A. 2005. The structure and kinematics of the southeastern Zagros fold-thrust belt; Iran: from thin-skinned to thick-skinned tectonics. *Tectonics* **24**, TC3007, doi:10.1029/2004TC001633, 19 pp.

MOLINARO, M., ZEYEN, H. & LAURENCIN, X. 2005. Lithospheric structure beneath the south-eastern Zagros Mountains, Iran: recent slab break-off. *Terra Nova* **17**, 1–16.

MORGAN, S. S. & LAW, R. D. 2004. Unusual transition in quartzite dislocation creep regimes and crystal slip systems in the aureole of the Eureka Valley-Joshua Flat-Beer Creek pluton, California: a case for anhydrous conditions created by decarbonation reactions. *Tectonophysics* **384**, 209–31.

OKUDAIRA, T., TAKESHITA, T., HARA, I. & ANDO, J. 1995. A new estimate of the conditions for transition from basal <a> to prism [c] slip in naturally deformed quartz. *Tectonophysics* **250**, 31–46.

PASSCHIER, C. W. 1988. The use of Mohr circles to describe non-coaxial progressive deformation. *Tectonophysics* **149**, 323–38.

PASSCHIER, C. W. & TROUW, R. A. J. 2005. *Microtectonics*. Berlin: Springer-Verlag.

PLATT, J. P. & BEHRMANN, J. H. 1986. Structures and fabrics in a crustal scale shear zone, Betic Cordillera, SE Spain. *Journal of Structural Geology* **8**, 15–33.

RALSER, S., HOBBS, B. E. & ORD, A. 1991. Experimental deformation of a quartz mylonite. *Journal of Structural Geology* **13**, 837–50.

RAMSAY, J. G. 1967. *Folding and Fracturing of Rocks*. New York: McGraw-Hill.

RAMSAY, J. G. & HUBER, M. I. 1987. *The Techniques of Modern Structural Geology, Vol. 2: Folds and Fractures*. London: Academic Press.

REGARD, V., BELLIER, O., THOMAS, J.-C., ABBASSI, M. R., MERCIER, J., SHABANIAN, E., FEGHHI, K. & SOLEYMANI, S. 2004. Accommodation of Arabia-Eurasia convergence in the Zagros-Makran transfer zone, SE Iran: a transition between collision and subduction through a young deformation system. *Tectonics* **23**, TC4007, doi: 10.1029/2003TC001599, 24 pp.

RING, U. & KASSEM, O. 2007. The nappe rule: why does it work? *Journal of the Geological Society, London* **164**, 1109–12.

SARKARINEJAD, K. & AZIZI, A. 2008. Slip partitioning and inclined dextral transpression along the Zagros Thrust System, Iran. *Journal of Structural Geology* **30**, 116–36.

SARKARINEJAD, K., FAGHIH, A. & GRASEMANN, B. 2008. Transpressional deformations within the Sanandaj-Sirjan Metamorphic Belt (Zagros Mountains, Iran). *Journal of Structural Geology* **30**, 818–26.

https://doi.org/10.1017/S0016756811000276 Published online by Cambridge University Press

SARKARINEJAD, K., GODIN, L. & FAGHIH, A. 2009. Kinematic vorticity flow analysis and 40Ar/39Ar geochronology related to inclined extrusion of the HP–LT metamorphic rocks along the Zagros accretionary prism, Iran. *Journal of Structural Geology* **31**, 691–706.

SARKARINEJAD, K., SAMANI, B., FAGHIH, A., GRASEMANN, B. & MORADIPOOR, M. 2010. Implications of strain and vorticity of flow analyses to interpret the kinematics of an oblique convergence event (Zagros Mountains, Iran). *Journal of Asian Earth Sciences* **38**, 34–43.

SEPEHR, M. & COSGROVE, J. W. 2005. Role of the Kazerun Fault Zone in the formation and deformation of the Zagros Fold-Thrust Belt, Iran. *Tectonics* **24**, TC5005, doi: 10.1029/2004TC001725, 13 pp.

SCHMID, S. M. & CASEY, M. 1986. Complete fabric analysis of some commonly observed quartz c-axis patterns. In *Mineral and Rock Deformation: Laboratory Studies – The Paterson Volume* (eds B. E. Hobbs & H. C. Heard), pp. 263–86. American Geophysical Union, Geophysical Monograph vol. **36**. Washington, DC, USA.

SHORT, H. A. & JOHNSON, S. E. 2006. Estimation of vorticity from fibrous calcite veins, central Maine, USA. *Journal of Structural Geology* **28**, 1167–82.

SIMPSON, C. & SCHMID, S. M. 1983. An evaluation of criteria to deduce the sense of movement in sheared rocks. *Geological Society of America Bulletin* **94**, 1281–8.

STÖCKLIN, J. 1974. Possible ancient continental margins in Iran. In *The Geology of Continental Margins* (eds C. E. Burk & C. L. Drake), pp. 873–88. New York: Spring-Verlag.

SULLIVAN, W. A. & LAW, R. D. 2007. Deformation path partitioning within the transpressional White Mountain shear zone, California and Nevada. *Journal of Structural Geology* **29**, 583–98.

TALEBIAN, M. & JACKSON, J. 2002. Offset on the Main Recent Fault of NW Iran and implications for late Cenozoic tectonics of the Arabia–Eurasia collision zone. *Geophysical Journal International* **150**, 422–39.

TATAR, M., HATZFELD, D. & GHAFORY-ASHTIYANI, M. 2004. Tectonics of the Central Zagros (Iran) deduced from microearthquake seismicity. *Geophysical Journal International* **156**, 255–66.

TIKOFF, B. & FOSSEN, H. 1995. The limitation of three-dimensional kinematic vorticity analyses. *Journal of Structural Geology* **17**, 1771–84.

TULLIS, J. 1977. Preferred orientation of quartz produced by slip during plane strain. *Tectonophysics* **39**, 87–102.

TULLIS, J., CHRISTIE, J. M. & GRIGGS, D. T. 1973. Microstructures and preferred orientations of experimentally deformed quartzites. *Geological Society of America Bulletin* **84**, 297–314.

VERNANT, P., NILFOROUSHAN, F., HATZFELD, D., ABBASI, M. R., VIGNY, C., MASSON, F., NANKALI, H., MARTINOD, J., ASHTIANI, A., BAYER, R., TAVAKOLI, F. & CHERY, J. 2004. Present–day crustal deformation and plate kinematics in the Middle East constrained by GPS measurement in Iran and northern Oman. *International Journal of Geophysics* **157**, 381–98.

VERNOOIJ, M. G. C., BROK, B. & KUNZE, K. 2006. Development of crystallographic preferred orientations by nucleation and growth of new grains in experimentally deformed quartz single crystals. *Tectonophysics* **427**, 35–53.

VISSERS, R. L. M. 1989. Asymmetric quartz c-axis fabrics and flow vorticity: a study using rotated garnets. *Journal Structural Geology* **11**, 231–44.

WALLIS, S. R. 1992. Vorticity analysis in a metachert from the Sanbagawa Belt, SW Japan. *Journal of Structural Geology* **14**, 271–80.

WALLIS, S. R. 1995. Vorticity analysis and recognition of ductile extension in the Sanbagawa Belt, SW Japan. *Journal of Structural Geology* **17**, 1077–93.

WALLIS, S. R., PLATT, J. P. & KNOTT, S. D. 1993. Recognition of syn-convergence extension in accretionary wedges with examples from the Calabrian Arc and the Eastern Alps. *American Journal of Science* **293**, 463–94.

WANG, Y., ZHANG, Y., FAN, W. & PENG, T. 2005. Structural signatures and 40Ar/39Ar geochronology of the Indosinian Xuefengshan tectonic belt, South China Block. *Journal of Structural Geology* **27**, 985–98.

XYPOLIAS, P. 2009. Some new aspects of kinematic vorticity analysis in naturally deformed quartzites. *Journal of Structural Geology* **31**, 3–10.

XYPOLIAS, P. & DOUTSOS, T. 2000. Kinematics of rock flow in a crustal-scale shear zone: implications for the orogenic evolution of the southwestern Hellenides. *Geological Magazine* **137**, 81–96.

XYPOLIAS, P. & KOUKOUVELAS, I. K. 2001. Kinematic vorticity and strain rate patterns associated with ductile extrusion in the Chelmos Shear Zone (External Hellenides, Greece). *Tectonophysics* **338**, 59–77.